The British Journal of Radiology, 85 (2012), 101–113

REVIEW ARTICLE

Gold nanoparticles as novel agents for cancer therapy

[1,2]S JAIN, MB, Bch, [3]D G HIRST, PhD and [1,2]J M O'SULLIVAN, MD

[1]*Northern Ireland Cancer Centre,* [2]*Centre for Cancer Research and Cell Biology, Queens University Belfast, and* [3]*School of Pharmacy, Queens University Belfast, Belfast, UK*

ABSTRACT. Gold nanoparticles are emerging as promising agents for cancer therapy and are being investigated as drug carriers, photothermal agents, contrast agents and radiosensitisers. This review introduces the field of nanotechnology with a focus on recent gold nanoparticle research which has led to early-phase clinical trials. In particular, the pre-clinical evidence for gold nanoparticles as sensitisers with ionising radiation *in vitro* and *in vivo* at kilovoltage and megavoltage energies is discussed.

Received 15 July 2010
Revised 22 December 2010
Accepted 5 January 2011

DOI: 10.1259/bjr/59448833

Nanotechnologies can be defined as the design, characterisation, production and application of structures, devices and systems by controlling shape and size at a nanometre scale [1]. Potential benefits of nanomaterials are well recognised in the literature and some commentators argue that nanotechnology promises to far exceed the impact of the Industrial Revolution, projecting to become a $1 trillion market by 2015 [2, 3]. In medicine, most interest is in the use of nanoparticles to enhance drug delivery with interest also in *in vitro* diagnostics, novel biomaterial design, bioimaging, therapies and active implants. Nanoparticles, according to the American Society for Testing and Materials (ASTM) standard definition, are particles with lengths that range from 1 to 100 nm in two or three dimensions [1]. The most studied nanoparticles are carbon nanotubes, gold nanoparticles (GNPs) and cadmium selenide quantum dots [4–6]. This review focuses on GNPs as promising novel agents for cancer therapy.

Gold nanoparticles

Common oxidation states of gold include +1 (Au [I] or aurous compounds) and +3 (Au [III] or auric compounds). GNPs, however, exist in a non-oxidised state (Au [0]). GNPs are not new; in the 19th century, Michael Faraday [7] published the first scientific paper on GNP synthesis, describing the production of colloidal gold by the reduction of aurochloric acid by phosphorous. In the late 20th century, techniques including transmission electron microscopy (TEM) and atomic force microscopy (AFM) enabled direct imaging of GNPs, and control of properties such as size and surface coating was refined [9]. Common methods of GNP production include citrate reduction of Au [III] derivatives such as aurochloric acid ($HAuCl_4$) in water to Au (0) and the Brust–Schiffrin method, which uses two-phase synthesis and stabilisation by thiols [9, 10]. In recent years there has been an explosion in GNP research, with a rapid increase in GNP publications in diverse fields including imaging, bioengineering and molecular biology (Figure 1). It is probable that this relates to a similar increase in the broader field of nanotechnology, increased governmental awareness and funding, and rapid progress in chemical synthesis and molecular biology [11].

GNPs exhibit unique physicochemical properties including surface plasmon resonance (SPR) and the ability to bind amine and thiol groups, allowing surface modification and use in biomedical applications [12]. Nanoparticle functionalisation is the subject of intense research at present, with rapid progress being made towards the development of biocompatible, multifunctional particles for use in cancer diagnosis and therapy [2]. For example, a multifunctional micellar hybrid nanoparticle containing metal nanoparticles for MRI detection, quantum dots for near infrared fluorescent imaging, polyethylene glycol (PEG) to increase circulation times, the tumour-specific F3 peptide for targeting and doxorubicin as a therapeutic payload has recently been developed. Efficacy has been demonstrated *in vitro* and *in vivo* in a mouse model implanted with human breast cancer cells [13].

There has been considerable debate about the mode of entry of GNPs into cells, with the most likely mechanism being non-specific receptor mediated endocytosis (RME) [14]. *In vivo*, even in the absence of functionalisation, nanoparticles passively accumulate at tumour sites that have leaky, immature vasculature with wider fenestrations than normal mature blood vessels [15]. This is known as the enhanced permeability and retention (EPR) effect. Difficulties in utilising the EPR effect for tumour drug delivery exist owing to the heterogeneity of tumour vasculature, particularly at the centre of poorly differentiated cancers, as well as particle detection and uptake by the reticuloendothelial system (RES) [16]. PEGylation is the most common method of reducing RES uptake, producing a hydrated barrier causing steric hindrance

Address correspondence to: Dr Suneil Jain, Centre for Cancer Research and Cell Biology, Queens University Belfast, 4 Malone Gate, Belfast BT9 6WG, UK. E-mail: suneiljain@hotmail.com

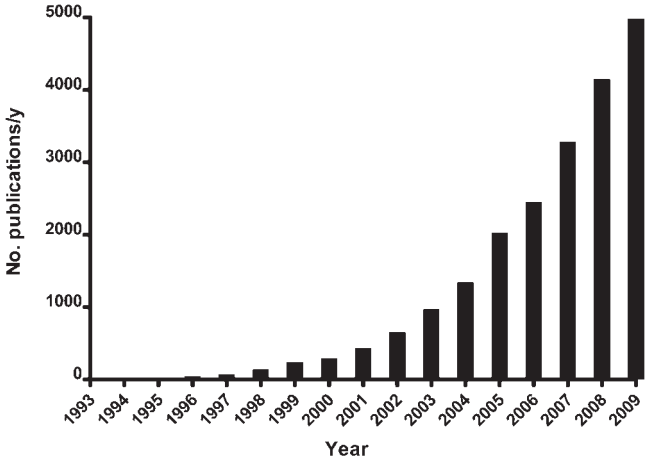

Figure 1. Number of gold nanoparticle papers published each year. Source: ISI Web of Knowledge. Available from: www.webofknowledge.com.

to the attachment of phagocytes [17]. The EPR effect combined with longer circulation times, often achieved by PEGylation, can increase concentrations of drug in tumours by 10–100-fold compared with the use of free drugs [18]. Further tumour targeting can be achieved by actively binding tumour-specific recognition molecules such as epidermal growth factor (EGF), transferrin, folic acid or monoclonal antibodies to nanoparticles [14, 19, 20]. Toxicity studies of GNPs have been conflicting, with interactions between GNPs and tissue at the cellular, intracellular and molecular levels remaining poorly understood [2]. While some studies have shown no cellular toxicity, other *in vitro* and *in vivo* studies have demonstrated cellular reactive oxygen species production, mitochondrial toxicity, cytokine release, apoptosis and necrosis [12, 21–27].

Gold nanoparticles as drug carriers

There is intense interest in modifying existing drugs to improve pharmacokinetics, thereby reducing non-specific side effects and enabling higher dose delivery to target tissues. An important demonstration of the potential of multifunctional GNPs for drug delivery was the use of 5-nm GNPs as a delivery vehicle, covalently bound to cetuximab, as an active targeting agent and gemcitabine as a therapeutic payload in pancreatic cancer [28]. The epidermal growth factor receptor (EGFR) is overexpressed in up to 60% of pancreatic cancers and the combination of cetuximab and gemcitabine has been investigated in Phase II trials of this disease [29]. Patra et al [30] demonstrated that high intratumoural gold concentrations ($4500\,\mu g\,g^{-1}$) could be achieved using this approach compared with $600\,\mu g\,g^{-1}$ with untargeted GNPs with minimal accumulation in the liver or kidney. The GNP–cetuximab–gemcitabine nanocomplex was superior to any of the agents alone or in combination *in vitro* and *in vivo.* Low doses of complex gemcitabine ($2\,mg\,kg^{-1}$) led to >80% tumour growth inhibition in an orthotopic pancreatic cancer model compared with 30% inhibition using the non-conjugated agents in combination [30].

Jiang et al [31] synthesised citrate-coated GNPs of controlled sizes ranging from 2 to 100 nm bound with multiple trastuzumab antibodies to enable targeting and cross-linking of human epidermal growth factor receptor (HER)-2 in human SK-BR-3 breast cancer cells. Larger nanoparticles had a greater protein-to-nanoparticle ratio than smaller, more curved particles, with more avid trastuzumab binding. In this study, the optimal size for nanoparticle cellular entry was 40–50 nm. Smaller particles dissociated from the cell membrane and larger particles appeared to reduce the membrane wrapping necessary for RME to occur. Furthermore, with 40 nm GNP–HER particles, the HER-2 receptor complex was noted to internalise to the cytoplasm, leading to a 40% reduction in surface HER-2, a process that does not occur with trastuzumab binding alone. This led to a reduced expression of downstream kinases including protein kinase B (Akt) and mitogen-activated protein kinase (MAPK) and a twofold increase in trastuzumab cytotoxicity. The concentration of GNPs used in this study was extremely low (fM concentrations), yet GNP–HER was clearly visualised in cytoplasmic lysosomes. This important work demonstrated that GNPs may not simply act as passive drug carriers, but may also influence drug–cell interactions and enhance therapeutic effects [31].

Gold nanoparticle thermal therapy

Hyperthermia is known to induce apoptotic cell death in many tissues and has been shown to increase local control and overall survival in combination with radiotherapy and chemotherapy in randomised clinical trials [32–34]. Hyperthermia is normally used in combination with other treatments, including radiotherapy, and can be delivered externally, interstitially or endoluminally with heat generation by radiofrequency waves, microwaves or ultrasound [35]. While normal tumour vasculature dilates to aid heat dissipation, tumour vasculature constricts, providing some tumour selectivity. However, overall, a lack of specificity for tumour tissue, difficulties in heating deep tumours to therapeutic temperatures and thermotolerance after initial treatment have limited the use of hyperthermia in cancer treatment [35].

Progress in nanomedical research offers the potential to specifically target metal nanoparticles to tumour cells. When an energy source such as a laser producing non-ionising electromagnetic radiation is applied, conversion to heat energy occurs in metal nanoparticles owing to electron excitation and relaxation [36]. Furthermore, lasers can be specifically tuned to the SPR frequency of nanoparticles, which varies with the size, shape and composition of the nanoparticle (Figure 2) [19]. Most research has used gold nanoshells, particles with 100-nm silica cores and a 15-nm gold coating, which shifts the resonance peak to the near infrared region (650–950 nm) where blood and tissue are maximally transmissive [37]. An *in vivo* study demonstrated 100 nm gold nanoshells maximally accumulated in SK-BR-3 human breast tumours 24 h after intravenous (IV) injection. When a laser tuned to the nanoshell resonance was applied, average tumour temperatures increased by 9°C in control mice, and 37°C in nanoshell-treated mice, with irreversible tissue damage in the nanoshell group. All mice in the nanoshell group survived 90 days with no evidence of tumour recurrence whereas all mice in the control group

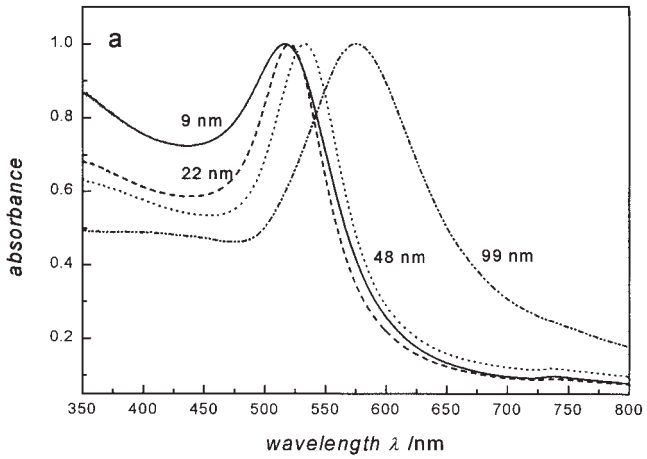

Figure 2. Absorption spectra of 9-nm, 22-nm, 48-nm and 99-nm gold nanoparticles demonstrating a change in surface plasmon resonance with particle diameter. Reproduced with permission from Link et al [87].

were euthanised by 20 days owing to uncontrolled tumour growth [38]. A similar approach used 110-nm PEGylated gold nanoshells and laser therapy to treat PC3 human prostate cancer xenografts. Nanoparticles were given intravenously to mice with laser therapy administered 18 h after nanoparticle exposure. A complete resolution of the tumour was noted in 93% of mice receiving gold nanoshells and laser, with no effects in tumours treated with laser alone (Figure 3) [39].

Some limitations to this technique continue to exist, particularly for treatment of deep seated tumours, as a laser will only penetrate several centimetres in soft tissue [36]. More methods to allow *in vivo* dose quantification of nanoshells to enable modification of laser doses need to be developed [37]. Furthermore, some studies have estimated that ~5000 nanoshells per cell will have to be delivered to achieve adequate heat production for coagulative necrosis to occur [40]. It remains to be seen whether this is achievable in clinical practice with more heterogeneous tumours than in pre-clinical models.

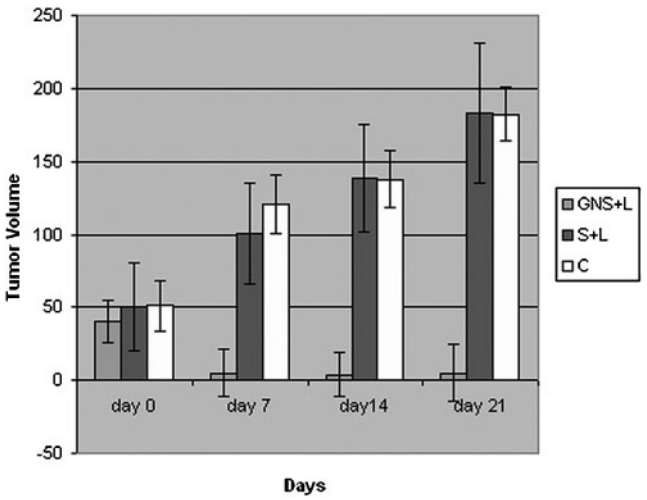

Figure 3. Tumour growth of human prostate cancer tumours in mice. C, control; GNS, gold nanoshells; L, laser; S, sham treated. Reproduced with permission from Stern et al [40].

Gold nanoparticles as contrast agents

The properties of GNPs, including small size, biocompatibility, high atomic number (high-Z) and the ability to bind targeting agents, mean that they have potential as contrast agents. Contrast materials such as iodine improve the definition of heavily vascularised tumours by increasing photoelectric photon absorption, increasing the accuracy of tumour diagnosis and staging and aiding volume and definition in radiotherpy planning [41].

At energies above 80 keV, the mass attenuation, $\frac{\mu}{\rho}$, of gold is higher than that of iodine, suggesting that better contrast would be achieved with gold. For instance, at 100 kV the $\frac{\mu}{\rho}$ for gold is $5.16\,cm^2\,g^{-1}$, for iodine it is $1.94\ cm^2g^{-1}$, for bone it is $0.186\,cm^2\,g^{-1}$ and for soft tissue it is $0.169\,cm^2\,g^{-1}$, so gold provides 2.7 times more contrast per unit weight than iodine [42]. 1.9 nm GNPs (Aurovist™; Nanoprobes, Inc., Yaphank, NY) have been used *in vivo*, demonstrating longer retention times and superior contrast to iodine with resolution of vessels as small as 100 μm [42]. They were intravenously injected into Balb/C mice implanted with EMT6 murine breast tumours and imaged with a 22-kVp mammography unit 2 min–24 h post-injection. Despite high initial blood concentrations of GNPs (10 mg ml^{-1} blood), no haematological or biochemical abnormalities were detected at 11 or 30 days post-injection. Quantitative pharmacodynamics demonstrated that GNPs were renally excreted with blood gold concentrations falling in a biphasic manner, with a 50% drop from 2 min to 10 min followed by a further 50% reduction from 15 min to 1.4 h. In contrast, tumour levels at 24 h were 64% of peak levels reached 15 min post-injection, suggesting nanoparticle extravasation into tumour tissue. Improved retention times and contrast could allow detection of smaller tumours at staging, aid image-guided radiotherapy and allow intratumoural GNP dose quantification.

While GNPs have the potential to improve contrast with structural imaging modalities, including CT and MRI, it is possible that functionalised GNPs could be useful in the field of molecular imaging to give *in vivo* information on the metabolic activity of cancer and the expression of molecular markers. In clinical use, positron emission tomography (PET) is the most used functional imaging modality and its benefits over standard imaging have been well demonstrated [43–45]. To date, CT has not been used as a molecular imaging modality because iodine cannot be conjugated to molecular proteins. Targeted nanoparticles, including superparamagnetic nanoparticles and GNPs, are now being developed to improve imaging with MRI and CT [46, 47]. For instance, GNPs were conjugated to UM-A9 antibodies, which bind to the A9 ($\alpha 4\beta 6$ intregin) protein which is overexpressed in many squamous cell head and neck cancers and correlates with metastatic potential [48]. In an *in vitro* study using CT imaging at 80 kVp, the CT attenuation (in Hounsfield units [HU]) was 168 HU in A9-expressing cells and 28 HU for non-expressing cells compared with non-exposed cells. This should be clinically meaningful because the HU for soft tissue is 50; however, this needs to be tested in *in vivo* studies [48]. A further study used GNPs chelated with gadolinium (Gd) to enable both CT owing to the high-Z gold and MRI owing to the Gd [49]. Again, greater absorption was noted

with GNPs than with iodine; HUs were equal with 10 mg ml^{-1} gold and 35 mg ml^{-1} iodine. The use of monochromatic X-rays at the European Synchrotron Radiation Facility (ESRF) enabled *in vivo* GNP dose quantification because gold produces characteristic X-ray spectra which is detectable using an ionisation chamber. The nanoparticles could be clearly imaged by both CT and MRI because they accumulated in the kidneys and bladder during renal excretion [49].

Gold nanoparticles as radiosensitisers

While GNP radiosensitisation has been observed in many studies, as discussed below, much work has been phenomenological and the mechanisms by which sensitisation occurs remain unclear. Most researchers have attributed GNP radiosensitisation to increased photoelectric photon absorption by high-Z materials at kilovoltage photon energies. However, if sensitisation occurs by this physical mechanism, effects would not be predicted to occur at clinically relevant megavoltage energies where Compton interactions are dominant [50]. For clinical translation and optimisation of effect, it would be beneficial to know the importance of GNP size, concentration, surface coating and distance from target material such as DNA on GNP-mediated radiosensitisation. Knowledge of the range and type of secondary energies released from the nanoparticle, such as short-range low-energy electrons, Auger electrons, photoelectrons or characteristic X-rays, and in turn how they vary with primary photon energies would also enable the development of more rationally designed GNPs for use with radiation. Some of the studies attempting to address these complex issues are discussed below. The concept of high-Z radiation dose enhancement has been known for many years [51]. This is a physical concept which makes use of the much greater photoelectric photon absorption in high-Z materials compared with soft tissue, particularly at kilovoltage photon energies, as demonstrated in Figure 4. Increased radiation side effects have been observed at the interface with high-Z materials owing to greater absorption of photons and deposition of energy in surrounding tissue from photoelectrons, Auger electrons and characteristic X-rays [52]. In therapeutic terms, if a high-Z material is present at higher concentrations in the tumour than in normal tissue, an improvement in the therapeutic index should be realised. Much work has been carried out with iodine (Z=53), a commonly used contrast agent; Matsudaira et al [53] demonstrated increased cell killing in an *in vitro* cell model with iodine added to growth medium. Santos Mello [54] achieved an intratumoural concentration of 5 mg ml^{-1} iodine and demonstrated reduced tumour growth delay in a rabbit model. These results led to a Phase I feasibility trial in which 8 patients received 3–5 weekly 5-Gy boosts with 140-kVp X-rays to intracranial metastases while undergoing whole brain radiotherapy with 40 Gy in 20 fractions over 4 weeks with 6-MV photons [55]. IV iodine contrast medium was administered prior to radiation and 140-kVp X-rays were delivered in 360° rotations in three planes to minimise skull dose. Brain metastases were measured on weekly CTs prior to and during treatment. Of eight patients treated, there was one complete response and four partial responses to therapy with no increase in early or late radiation side effects.

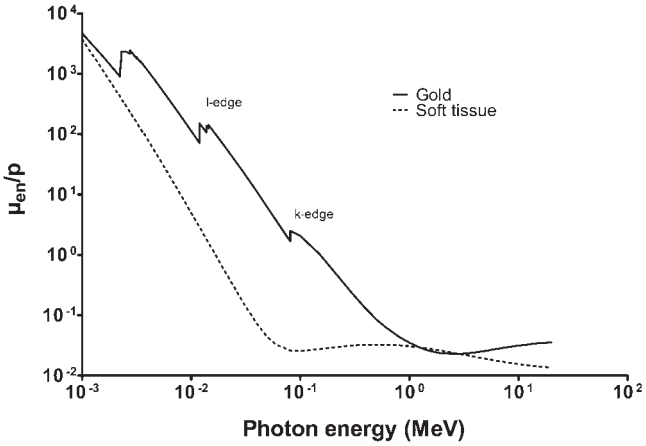

Figure 4. The relationship of mass attenuation coefficients of soft tissue and gold with increasing photon energy (source: National Institute Standards and Technologies).

DNA plasmid studies

The DNA plasmid model is a relatively simple system that allows the study of radiation-induced DNA damage and chemical-free radical effects [56]. Plasmid DNA refers to double stranded extrachromosomal DNA which ranges from a few hundred to a few thousand base pairs in length and is normally present in bacteria. This model allows control over the environment that the DNA is exposed to as the radical scavenging conditions can be varied, enabling assessment of the direct and indirect effects of radiation. The plasmid model allows measurement of sensitisation without the biological interactions of GNPs with cells and without the impact of DNA repair.

In a modelling and plasmid study, Carter et al [57] examined the distribution of energy release from nanoparticles to determine how close to targets such as DNA they need to be for sensitisation to occur. This question is important because if energy release is on the nanoscale, then efforts should be made to target the nanoparticles to the cell nucleus using methods such as the attachment of a nuclear localisation signal (NLS). This group modelled 3-nm GNPs intercalated to plasmid DNA in water irradiated with 100-kVp X-rays. The study showed that while some energy was released by long-range photoelectrons (which can travel for several micrometres), most was in the form of low energy electrons (LEEs) (<100 eV) with ranges of only a few nanometres. They confirmed these modelling results using the plasmid model with increasing concentrations of tris(hydroxymethyl)aminomethane (TRIS) as a free radical scavenger. At low scavenging concentrations, no GNP enhancement occurred because free radicals produced by photon interaction with water-dominated DNA damage. As TRIS concentrations were increased and the range of radicals in water reduced, and at physiological scavenging conditions (~100 mM TRIS), where radical range is in the order of 5 nm, enhancement was maximal at ~150% (Figure 5). Under these conditions, only radicals produced very close to DNA, either by water or GNPs, would cause damage, thus confirming the nanoscale nature of GNP energy release. Interestingly, with 6-nm GNPs the number of LEEs was significantly reduced because many electrons were not released from the nanoparticle.

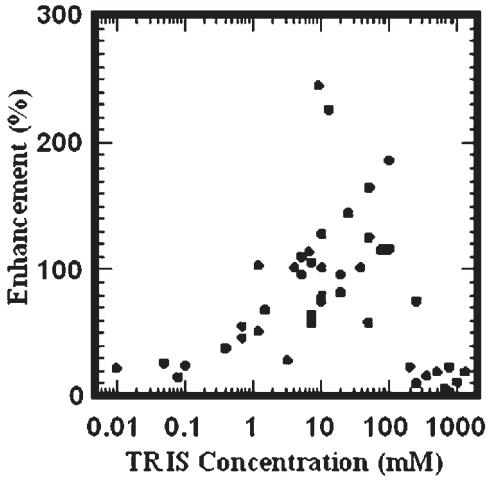

Figure 5. The influence of the free radical scavenger tris(hydroxymethyl)aminomethane on DNA plasmid-bound gold nanoparticle (GNP) radiosensitisation. Enhancement increases with concentration as more water radicals are scavenged. At concentrations >100 mM, enhancement falls as GNP-produced radicals are also scavenged. Reproduced with permission from Carter et al [57].

Boudaiffa et al [58] used the DNA plasmid model to demonstrate that very LEEs (<20 eV), which do not have enough energy to cause direct ionisation of DNA or other molecules (such as water), were capable of causing DNA damage. These LEEs are the most abundant form of secondary species produced when photons interact with matter (most probable energy: 10 eV) and have a range in matter of 1–10 nm. They postulated that this damage occurred through a process called dissociative electron attachment (DEA) whereby the incident electrons attach to basic components of DNA, resonate and form a transient molecular anion which can lead to fragmentation of small molecules. These products subsequently react with other components of DNA to cause single-strand breaks (SSBs) and double-strand breaks (DSBs). Zheng et al [59] used this model to examine radiosensitisation with both GNPs and cisplatin. 5 nm GNPs at a concentration of 12 μm were non-covalently bound to plasmid DNA and irradiated with 60 keV electrons in a vacuum [59]. With a GNP-to-plasmid ratio of 2:1, DSB formation increased by a factor of 2.6. In a separate experiment, GNP–plasmid complexes of different thicknesses (10 nm and 2900 nm) were irradiated with much greater DNA damage observed in the thin film, suggesting that low-range LEEs caused most of the damage. Because secondary LEEs are produced by photons of all energies and are responsible for much biological damage, this model suggests that enhancement would also be seen at megavoltage photon energies. This work was extended by chemically linking cisplatin to plasmid DNA irradiated with 60-keV electrons in the presence and absence of GNPs. Zheng and Sanche [60] demonstrated that radiation damage was enhanced by a factor of 7.5 when two cisplatin molecules and one GNP were bound to each plasmid. Clearly this level of enhancement with such low concentrations of GNPs cannot simply relate to increased photoelectric absorption and this group attributed the magnitude of this effect to DEA [60].

Butterworth et al [56] examined the impact of size and scavenging conditions on radiosensitisation. A dose enhancement factor (DEF) of 2 was noted for SSB and DSB with 50 μg ml^{-1} of 5-nm GNP in a 10-mM TRIS buffer with 160-kVp X-rays. Unexpectedly, GNPs had radioprotective effects in low scavenging conditions (phosphate-buffered saline), suggesting that GNPs themselves may have some free radical scavenging properties. Gold microparticles of 1.5 μm diameter caused some enhancement with SSB and DSB DEFs of 1.41 and 1.12, respectively. 5 nm GNPs at the same gold concentration gave SSB and DSB DEFs of 2.29 and 1.25, respectively. The DNA plasmid model can give useful information about the mechanisms by which sensitisation can occur and guide the design of *in vitro* and *in vivo* GNP experiments.

Monte Carlo modelling studies

Cho [50] modelled the effects of GNPs with an iridium-192 source, kilovoltage and megavoltage photon energies. With 140-kVp X-rays and a uniform distribution of 7 mg ml^{-1} GNPs, a DEF of 2.11 was predicted. However at megavoltage energies, predicted physical enhancement was extremely low; for example, a physical dose enhancement of 1–7% was predicted with 4-MV and 6-MV photons with gold concentrations ranging from 7 to 30 mg ml^{-1}. For an iridium-192 source placed in contact with tumour cells, dose enhancements of 8–30% were predicted with GNP concentrations ranging from 7 to 30 mg ml^{-1}. If gold was non-uniformly distributed in the tumour, as may be expected, or accumulated near cellular targets (*e.g.* DNA), estimation of dose on the nanoscale would be required. To date, these Monte Carlo (MC) studies have not been performed owing to MC code and computational limitations.

A further modelling study compared GNP dose enhancement with a range of X-ray energies, including commonly used brachytherapy radioisotopes, demonstrating, as expected, that high-Z materials at lower photon energies would be predicted to yield the greatest physical enhancement [61]. It was noted that even in the superficial and orthovoltage kilovoltage range, where photoelectric interactions are dominant, significant enhancement would occur only if uniform GNP concentrations were greater than 1 mg ml^{-1}. Other MC modelling studies have assessed the feasibility of using GNPs with kilovoltage energy photons and multiple fields or rotational arc techniques to treat tumours at different depths. McMahon et al [62] generated a figure of merit to account for increased radiation absorption in tumours loaded with 1% GNPs, demonstrating that tumours up to 4 cm deep could be preferentially treated with kilovoltage photons. However, this study did not consider increased radiation dose to skin owing to loss of radiation build-up, which may be dose-limiting. Furthermore, a commercial kilovoltage X-ray unit with the ability to deliver intensity-modulated radiation is unlikely to be developed. Other studies examined the feasibility of using 150-kVp radiation to treat prostate cancers loaded with a uniform distribution of 1% gold [63]. While it was possible to deliver 72 Gy to the prostate without exceeding tolerance doses to organs at risk (including rectum, bladder,

femoral heads and skin), the dose–volume histograms were inferior to those achieved using a 15-MV linear accelerator. Furthermore, variations in the gold concentration within the tumour, as will occur clinically, led to a significant degradation in the organs at risk dose–volume histograms.

Patients with localised prostate cancer are often treated with brachytherapy using iodine-125 (I-125) or palladium-103, which emit γ-rays of maximum energy 35 keV and 21 keV, respectively. Cho et al [64] specifically modelled I-125 brachytherapy seeds in tumours exposed at 0–18 mg g^{-1} GNPs. DEFs of 1.68 were noted at a distance of 1 cm from the I-125 source when 7 mg ml^{-1} GNP were used. The study assumed uniform atomic gold distribution throughout the tumour. The photoelectron fluence increased by up to two orders of magnitude, particularly at energies of <20 keV owing to interactions with the l-edge and m-edge of gold. The fluence of photoelectrons and Auger electrons was similar; however, the photoelectrons contributed significantly more to local dose deposition than the Auger electrons (by a factor of three). In summary, MC modelling suggests that meaningful physical dose enhancement will be observed only at kilovoltage photon energies where the photoelectric cross-section is dominant, even when high doses of GNPs are used.

In vitro *studies*

Initial biological studies of gold dose enhancement were carried out with monolayers of C3H 10T1/2 cells murine cells grown on thin layers of gold foil. Using physical dosimetry, Regulla et al [65] demonstrated massive DEFs of 55–114 when detectors were placed next to gold foil encased in polymethylmethacrylate (PMMA) and irradiated with mean X-ray energies of 33–100 kV. With 80 kV X-rays, the secondary radiation decreased exponentially with the distance from the gold foil and was negligible at 30 μm. In biological experiments with cell monolayers, biological enhancement factors of 30 were observed for cells placed 2 μm away from gold foil. Because gold foil has limited therapeutic potential, further important work by Herold et al [66] examined enhancement with 3 μm diameter gold microparticles *in vitro* and *in vivo*. The dose enhancement with 1% gold microparticles in solution without cells was determined using chemical Fricke dosimetry and observed to be 1.42 for 200 kVp X-rays. Interestingly, Cs-137, which produces 662 keV photons, showed no strengthening of dose. At this energy, Compton effects are dominant and while dose in front of high-Z materials will increase owing to back-scatter, dose behind the material will reduce because of shielding with no net overall enhancement. Clonogenic survival in three cell lines of varying radiosensitivity, CHO-K1, DU-145 and EMT-6, with radiation energies of 100 kVp and 240 kVp, and Cs-137 was then examined. For 200-kVp X-rays, the overall DEF was 1.43; for Cs-137, a small non-significant enhancement was observed. Linear quadratic fits demonstrated increases in both the alpha and beta components of the survival curve. *In vivo/ex vivo* studies with direct injection of 1% microparticles into implanted EMT-6 tumours demonstrated a reduction in plating efficiency from 0.248 in controls to 0.149 in microparticle-exposed tumours (p=0.06). Microscopy showed that particles were poorly distributed throughout the tumour interstitium and were not observed in areas of tightly packed tumour cells. Clearly, particles of this size are too big to enter cells, which have a typical diameter of 10-15 μm.

Chithrani et al [67] investigated the impact of GNP size, concentration and radiation energy on *in vitro* radiosensitisation in Hela cells. Previous studies have demonstrated that 50 nm GNPs were taken up in cells in greater numbers than 14 nm or 74-nm GNPs, although the greatest amount of gold was delivered with 74-nm particles [14]. In keeping with this, the greatest radiosensitisation was observed with 50-nm GNPs when compared with 14-nm and 74-nm particles with 220-kVp X-rays (DEFs were 1.43, 1.2 and 1.25, respectively). The magnitude of radiosensitisation was found to be GNP concentration dependent with 50-nm GNPs and correlated with the number of intracellular nanoparticles, but not the total amount of intracellular gold when different-sized nanoparticles were considered. Rahman et al [68] studied the *in vitro* radiosensitising effects of 1.9-nm GNPs (Aurovist), which have also been used in *in vivo* studies [26, 68, 69]. Bovine aortic endothelial cells (BAEC) were exposed to high concentrations of GNPs (up to 1 mM) prior to irradiation with 80-kVp or 150-kVp X-rays. A cell proliferation assay was used to calculate gold alone, toxicity and radiosensitisation. GNPs caused up to 30% loss of cell proliferation when used alone and large radiation DEFs (up to 24) with 80-kVp X-rays. Dose enhancement was reduced with 150-kVp X-rays and MeV electrons with DEFs of 1.4 and 2.9, respectively. An *in vitro* study used 30-nm citrate or thioglucose-coated GNPs with DU145 cells irradiated with 200-kVp X-rays after 24 h GNP exposure [70]. A threefold increase in GNP uptake was observed in glucose-capped GNPs, with a reduction in cellular proliferation with exposure to either GNP preparation. The combination of GNPs with radiation was largely additive, with glucose-capped GNPs having a greater effect on cellular proliferation than citrate GNPs with 2-Gy radiation (46% and 30.6% reduction, respectively). A further study compared thioglucose and cysteamine-capped 10.8-nm GNPs in MCF7 breast cancer and MCF10a normal breast cells irradiated with 200-kVp, caesium-137 or cobalt-60 radiation [71]. The toxicity of GNPs alone was <10% with cell proliferation assays. A single radiation dose clonogenic assay was carried out with thioglucose GNPs, which demonstrated a supra-additive effect with GNPs and radiation. Further work from this group looked at the mechanisms of GNP sensitisation in DU145 cells exposed for 2 h to 15-nm 10.8-nm thioglucose GNPs and irradiated with 2-Gy Cs-137 γ-rays [72]. Clonogenic survival, as measured by the surviving fraction at 2 Gy (SF_2), fell from 1.0 to 0.38 when GNPs were combined with radiation and a corresponding increase in apoptotic cells was observed. The proportion of cells in the radiosensitive G2/M phase of the cell cycle increased from 18.4% in untreated cells to 29.9% when radiation was combined with GNPs. A further study used high concentrations of 20-nm GNPs: 0.25–2 mM (50–400 mg ml^{-1}) in combination with 6-MeV electrons, demonstrating radiosensitisation with CT-26 mouse colorectal cell lines [73]. These studies are summarised in Table 1.

While some cancer patients are treated with kilovoltage radiation with brachytherapy, intra-operative radiotherapy, radionuclide therapy and superficial X-ray

Table 1. *In vitro* studies of GNP radiosensitisation with ionising radiation

	Year	GNP	GNP conc.	Time to RT	Cell line	Uptake (GNP cell^{-1})	GNP distribution	GNP toxicity	Radiation	Effect
Zhang et al [70]	2008	30 nm	15 nM	24 h	DU145	2.06×10^4	Lysosomes	13.5% LP at 24 h	200 kVp	LP 30.57%
			15 nM			6.73×10^4		17.8% LP at 24 h	200 kVp	LP 46%
Kong et al [71]	2008	10.8 nm	15 nM	2 h	MCF7, MCF10a	2.96×10^4		~5% at 24 h	200 kVp/662 keV/1.2 MV	LP 63.5%/60%/60%
			15 nM, 3.85 nM	2 h		1.19×10^5	Cell membrane	~10% at 24 h	200 kVp/662 keV/1.2 MV	LP 31.7%/60%/60%
Roa et al [72]	2009	10.8 nm	15 nM	2 h	DU145	NR		0%	Cs-137 (662 keV)	SF_2=0.38
Chang et al [79]	2008	13 nm	11 nM (180 μg ml^{-1})	18 h	B16F10	NR	Cytoplasm	NR	6 MeV electrons	DEF ~1.02
Chithrani et al [67]	2010	14 nm	1 nM (1 × 10−3%)	24 h	Hela	1.5×10^3		NR	220 kVp	DEF 1.2 (at 10% survival)
		74 nm	1 nM (1 × 10−3%)	24 h		6.0×10^3			220 kVp	DEF 1.25
		50 nm	1 nM (1 × 10−3%)	24 h		3.0×10^3			105 kVp	DEF 1.66
		50 nm		24 h					220 kVp	DEF 1.43
		50 nm		24 h					6 MV	DEF 1.17
		50 nm		24 h					Cs-137 (662 keV)	DEF 1.18
Rahman et al [68]	2009	1.9 nm	0.25–1 mM		BAEC	NR	Cytoplasm	17% at 0.25 mM	80 kV	DEF 20 (0.5 mM)
			0.25–1 mM						150 kV	DEF 1.4 (0.5 mM)
			0.25–1 mM						6 MeV electrons	DEF 2.9 (0.5 mM)
			0.25–1 mM						12 MeV electrons	DEF 3.7 (0.5 mM)
Chien et al [73]	2007	20 nm	0.0125–2 mM	24 h	CT-26	NR	Cytoplasm	50% 1 mM	6 MeV electrons	DEF ~1.19 (1 mM)
Liu et al [77]	2010	6.1 nm	0.4–1 mM		CT-26, EMT-6				6.5 keV synchrotron	DEF ~2 (at 50% survival, 0.5 mM)
									160 kVp	DEF ~1.1 (at 50% survival, 0.5 mM)
									6 MV	DEFv ~1 (at 50% survival, 0.5 mM)

BAEC, bovine aortic endothelial cells; DEF, dose enhancement factor; GNP, gold nanoparticle; LP, loss of proliferation; NR, not reported; RT, radiotherapy; SF_2, surviving fraction at 2 Gy.

therapy, most patients are treated with megavoltage photons produced by a clinical linear accelerator [74, 75]. Two recent studies have reported *in vitro* GNP sensitisation at megavoltage photon energies. One study used Hela cells exposed to 50-nm citrate-coated GNPs for 24 h with DEFs of 1.66, 1.43 and 1.17 observed with 105-kVp, 220-kVp and 6-MV X-rays, respectively [76]. Radiosensitisation was less at megavoltage energies, but far greater than MC simulations predicted. A further study used CT-26 murine cancer cells treated with high concentrations (500 μM) of 6.1-nm PEGylated GNPs for 48 h. Cells were irradiated with 8-keV, 160-kVp and 6-MV X-rays, achieving DEFs, of ~1.44, 1.1 and 1.32, respectively [77]. Radiosensitisation with megavoltage electrons has been noted in other studies, with Rahman et al [68] reporting DEFs of 2.9 and 3.7 using 0.5 mM concentrations of 1.9 nm GNPs at 6-MeV and 12-MeV electron energies, respectively. These studies, together with increasing evidence of GNP biological activity, suggest that the mechanism of radiosensitisation may involve more than simply high-Z dose enhancement.

In vivo *studies*

Despite the rapid increase of GNP publications in recent years and an increasing number of *in vivo* studies investigating the uptake and distribution of GNPs, there remains a paucity of studies of *in vivo* radiosensitisation with GNPs. These studies will be critical for successful translation of this approach to the clinic.

1.9 nm GNPs (Aurovist) in combination with 250 kVp radiation were shown to prolong survival in tumour-bearing mice [26]. In the first experiment, Balb/C mice bearing EMT-6 murine breast cancer tumours received a single dose of 30 Gy using 250-kVp radiation alone or in combination with high concentrations of GNPs (1.35 g of Au kg^{-1}) injected intravenously 5 min prior to irradiation. Radiation alone induced tumour growth delay; however, radiation and GNPs actually led to a dramatic reduction in tumour growth when assessed 1 month after treatment. GNPs alone had no effect on tumour growth (Figure 6). This encouraging result prompted a second experiment with longer follow up in which mice received a slightly lower radiation dose (26 Gy) alone or with 1.35 g of Au kg^{-1} or 2.7 g of Au kg^{-1} GNPs. 50% (1.35 g of Au kg^{-1}) and 86% (2.7 g of Au kg^{-1}) of GNP-exposed mice treated with radiation survived for 1 year compared with 20% with radiation alone and 0% with gold only or no treatment ($p<0.01$) (Figure 7). Pharmacokinetics showed gold concentrations peaked in tumour vasculature 7 min post-injection. GNPs cleared twice as fast from surrounding muscle tissue as from the tumour. GNPs appeared to accumulate more in the tumour periphery than in the main tumour mass, with concentrations peaking at 6.5 mg of Au g^{-1} of tumour. GNP concentrations shortly after injection were higher in tumours than in the liver; however, more detailed information on biodistribution and GNP tissue extravasation is required. In this study, surviving mice remained alive for 1 year after treatment with no obvious long-term toxicities.

A study investigated 5-nm GNPs coated with Gd in mice bearing MC7-L1 murine breast cancer cells [78]. *In vitro*, these GNPs showed marked cytotoxicity with a 55% loss in colony formation in the absence of radiation and no

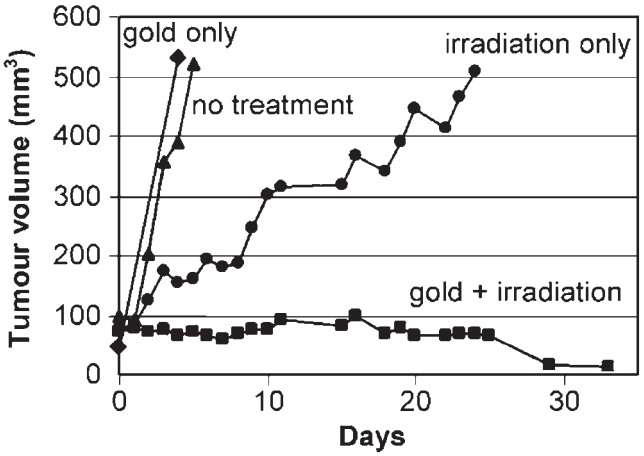

Figure 6. Triangles: tumour growth after no treatment ($n=12$); diamonds: gold only ($n=4$); circles: radiation only (30 Gy, $n=11$); squares: gold and radiation (n=10). Reproduced with permission from Hainfeld et al [26].

radiosensitisation at concentrations up to 5 μM. The Gd enabled *in vivo* monitoring of GNP biodistribution and demonstrated maximum tumour uptake at 10 min with a tumour-to-muscle ratio of 3:1 when 13.5 mg of gold was injected. Mice were exposed to GNPs alone or in combination with 10 Gy 150 kVp X-rays 20 min after GNP injection. There was no difference in survival times in the GNP and radiation group compared with radiation alone, with median survivals of 17 days and 14 days, respectively. Chang et al [79] used 13-nm citrate-coated GNPs in a mouse model with B16F10 murine melanoma cells. Interestingly, little effect was noted in *in vitro* clonogenic assays, with GNP concentrations of 180 μg ml^{-1} achieving DEFs of 1.08. Significant *in vivo* tumour growth delay and increased survival were noted when 36 mg kg^{-1} GNPs were injected 24 h before irradiation with 25 Gy of 6-MeV electrons produced by a linear accelerator. The median survival was shorter than in the Hainfeld study, with median survivals of 20 days for non-irradiated mice, 5 days for radiation only and 65 days for GNP-radiation groups. In a separate experiment, significant increases in apoptosis were observed in mice receiving GNPs plus radiation compared with radiation alone, as measured by

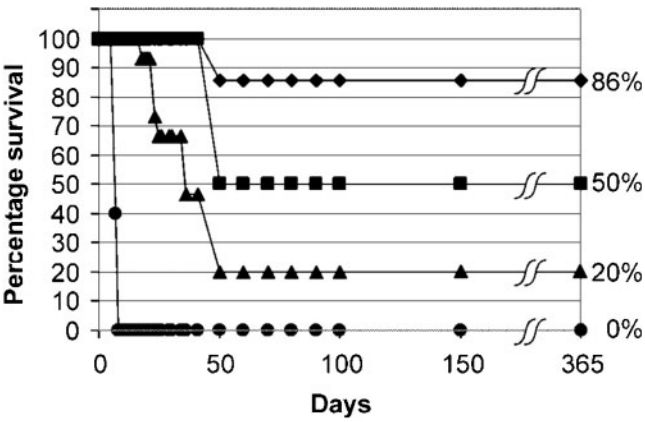

Figure 7. Kaplan–Meier survival. Circles: no treatment or gold alone; triangles: radiation only; squares: radiation after 1.35 g of Au kg^{-1} gold nanoparticles; diamonds: radiation after of 2.7 g of Au kg^{-1} injection. Reproduced with permission from Hainfeld et al [26].

Table 2. *In vivo* studies of GNP radiosensitisation with ionising radiation

Study	Year	GNP	GNP dose	Time to RT	Cell line	Radiation	Dose (Gy)	Outcome measure	Group	Outcome	*p*-Value
Hainfeld et al [26]	2004	1.9 nm GNP	1.35 g kg^{-1}	5 min	EMT-6	250 kVp	26–30	OS at 1 y	GNP only	0%	
			0 g kg^{-1}						RT only	20%	
			1.35 g kg^{-1}						GNP+RT	50%	
			2.7 g kg^{-1}						GNP+RT	86%	0.01
Hebert et al [78]	2008	5 nm DTDTPA-Gd	0 g kg^{-1}	20 min	MC7-L1	150 kVp	10	Median survival	Control	9 days	
			0.675 g kg^{-1}						GNP only	13 days	
			0 g kg^{-1}						RT only	14 days	
			0.675 g kg^{-1}						GNP+RT	17 days	NR
Chang et al [79]	2008	13 nm citrate GNP	0 g kg^{-1}	24 h	B16F10	6 MeV	25	Median survival	Control	20 days	
			0.036 g kg^{-1}						GNP only		
			0 g kg^{-1}						RT only	55 days	
			0.036 g kg^{-1}						GNP+RT	65 days	<0.05
Hainfeld et al [69]	2010	1.9 nm GNP	0 g kg^{-1}	5 min	SCCVII	68 keV	42	Doubling time (OS)	RT only	53 days (25%)	
			1.9 g kg^{-1}						GNP+RT	76 days (67%)	
			0 g kg^{-1}			68 keV	30		RT only	45 days (14%)	
			1.9 g kg^{-1}						GNP+RT	44 days (14%)	
			0 g kg^{-1}			157 keV	44		RT only	29 days (0%)	
			1.9 g kg^{-1}						GNP+RT	31 days (29%)	<0.05
			0 g kg^{-1}			157 keV	50.6		RT only	31 days (0%)	
			1.9 g kg^{-1}						GNP+RT	49 days (38%)	<0.05

DTDTPA, dithiolated diethylenetriaminepentaacetic; Gd, gadolinium; GNP, gold nanoparticle; NR, not reported; OS, overall survival; RT, radiotherapy.

the terminal deoxynucleotidyl transferase dUTP nick end-labelling assay. This study is important as it used lower GNP doses with clinically relevant electron energies. Biodistribution studies showed gold accumulated in tumours after 24 h (74.24 $\mu g\,mg^{-1}$ tissue), but also in the liver and spleen (147 $\mu g\,ml^{-1}$ and 350 $\mu g\,ml^{-1}$, respectively), suggesting uptake by the RES, which may be reduced by PEGylation or active targeting. Hainfeld et al [69] have recently published a further *in vivo* study using 1.9 nm GNPs. In this study, a highly radioresistant murine squamous cell carcinoma, SCCVII, was used in mice irradiated with filtered photons produced in a synchrotron. Using 68-keV photons, significant tumour growth delay and long-term tumour control were observed when 1.9 g of $Au\,kg^{-1}$ were combined with 42-Gy radiation compared with radiation alone. This effect was not observed when 30 Gy of radiation was used. Similarly with 157-keV photons, more effect was observed with GNPs combined with 50.6 Gy than with 44 Gy. There was no analysis of GNP tumour uptake or distribution in this study. The results of *in vivo* GNP studies are summarised in Table 2.

Gold nanoparticle clinical trials

Nanomedical research remains relatively immature and the full clinical impact is not yet known. Many new nanocomplexes are being developed for cancer therapy and there is a need to translate these products to clinical trials in a timely but safe manner. The Nanotechnology Characterisation Laboratory (NCL) was formed in 2004 by a formal collaboration between three US federal organisations: the National Cancer Institute, the US Food and Drug Administration and the National Institute of Standards and Technology [80]. It performs and standardises the pre-clinical characterisation of nanomaterials intended for cancer therapeutics. The NCL will perform physicochemical *in vitro* and *in vivo* characterisation and has tested over 180 nanomaterials to date.

The first GNP therapy to have reached early-phase clinical trials is CYT-6091, 27-nm citrate-coated GNPs bound with thiolated PEG and tumour necrosis factor-α (TNF-α) (Aurimmune; CytImmune Sciences, Rockville, MD), which has the dual effect of increasing tumour targeting and tumour toxicity [81]. TNF-α is a multifunctional cytokine known to be both cytotoxic and immunomodulatory. Previous clinical trials of TNF-α demonstrated dose-limiting toxicities of hypotension and nausea at concentrations of 225 $\mu g\,m^{-2}$, which limited more widespread clinical use [82]. Recent preclinical studies compared TNF alone with citrate GNP–TNF complexes. While TNF-related toxicity was improved, unacceptable uptake occurred *via* the RES. There was a dramatic improvement in tumour specificity when PEG-thiol was added with active tumour uptake, plateauing at 6 h, and a gradual reduction in liver and spleen concentrations occurred over the same time [83]. A Phase I study of CYT-6091 commenced in 2005, enrolling 29 patients with solid cancers unresponsive to conventional therapies. Dose levels of 50–600 $\mu g\,m^{-2}$ TNF were administered, with no dose-limiting toxicities observed. Grade II fever, controllable with the use of antipyretics, was the main side effect. The highest dose of TNF used in this trial was more than three times the maximally tolerated dose in historic TNF trials. One partial response and three stable diseases were observed, with further trials in combination with chemotherapy now planned [84]. Intracellular GNPs were detectable in post-treatment tumour biopsies, but not in normal tissue. Pre-clinical studies of CYT-6091 bound with paclitaxel (known to synergise with TNF) have demonstrated 10 times more paclitaxel uptake in solid tumours than paclitaxel alone [81].

A single-dose pilot study of AuroShell® particles (Nanospectra Biosciences, Inc., Houston, TX) given intravenously to patients with recurrent or refractory head and neck cancer for photothermal therapy plans to recruit 15 patients [85]. Patients will receive IV AuroShell particles followed by one or more interstitial illuminations with an 808-nm laser. Post-treatment biopsies will assess nanoparticle uptake in tumours using neutron-activated analysis [86].

Summary

GNPs have many properties that are attractive for use in cancer therapy. They are small and can penetrate widely throughout the body, preferentially accumulating at tumour sites owing to the EPR effect. Importantly, they can bind many proteins and drugs and can be actively targeted to cancer cells overexpressing cell surface receptors. While they are biocompatible, it is clear that GNP preparations can be toxic in *in vitro* and *in vivo* systems. GNPs have a high atomic number, which leads to greater absorption of kilovoltage X-rays and provides greater contrast than standard agents. They resonate when exposed to the light of specific energies, producing heat that can be used for tumour-selective photothermal therapy. GNPs have been shown to cause radiosensitisation at kilovoltage and megavoltage photon energies. The exact mechanism remains to be seen but it may be physical, chemical or biological.

Many questions need to be answered before GNP complexes enter routine clinical use. The factors that affect GNP pharmacokinetics, biodistribution and *in vivo* toxicity need to be clarified. Targeted GNPs need to exit tumour vasculature, cross the tumour interstitium, enter cells and potentially exit lysosomes to be effective *in vivo*. They must be able to reach hypoxic cells, which lie far from the vasculature, because these cells are known to be both chemoresistant and radioresistant. Long-term studies are required to evaluate the toxicity and mutagenic potential of GNP RES uptake, because particles may remain in cells for many months. A standard approach for physicochemical characterisation and pre-clinical testing needs to be implemented, and this process is being aided by the NCL. Rigorous quality assurance needs to ensure minimal batch-to-batch variation, especially when production is scaled up for clinical use. There is huge potential to use nanoparticles in cancer therapy. With intense global interest in nanotechnology and particularly in nanomedicine, it is likely that many of these questions will be addressed in the near future.

References

1. ASTM International. E 2456-06 Terminology for nanotechnology. West Conshohocken, PA: ASTM International, 2006.

2. Nel A, Xia T, Madler L, Li N. Toxic potential of materials at the nanolevel. Science 2006;311:622–7.
3. Service RF. American Chemical Society meeting. Nanomaterials show signs of toxicity. Science 2003;300:243.
4. Magrez A, Kasas S, Salicio V, Pasquier N, Seo JW, Celio M, et al. Cellular toxicity of carbon-based nanomaterials. Nano Lett 2006;6:1121–5.
5. Chang E, Thekkek N, Yu WW, Colvin VL, Drezek R. Evaluation of quantum dot cytotoxicity based on intracellular uptake. Small 2006;2:1412–17.
6. Daniel MC, Astruc D. Gold nanoparticles: assembly, supramolecular chemistry, quantum-size-related properties, and applications toward biology, catalysis, and nanotechnology. Chem Rev 2004;104:293–346.
7. Faraday M. Experimental relations of gold and other metals to light. Philos Trans 1857;147:145–81.
8. Eigler DM, Schweizer EK. Positioning single atoms with a scanning tunnelling microscope. Nature 1990;344:524–6.
9. Turkevitch J, Stevenson PC, Hillier J. Nucleation and growth process in the synthesis of colloidal gold. Discussion. Faraday Soc 1951;11:55–75.
10. Brust M, Walker M, Bethell D, Schiffrin DJ, Whyman RJ. Synthesis of thiol-derivatized gold nanoparticles in a two-phase liquid-liquid system. J Chem Soc Chem Commun 1994;801–2.
11. Chen H, Roco MC, Li X, Lin Y. Trends in nanotechnology patents. Nat Nano 2008;3:123–5.
12. Shukla R, Bansal V, Chaudhary M, Basu A, Bhonde RR, Sastry M. Biocompatibility of gold nanoparticles and their endocytotic fate inside the cellular compartment: a microscopic overview. Langmuir 2005;21:10644–54.
13. Park JH, von Maltzahn G, Ruoslahti E, Bhatia SN, Sailor MJ. Micellar hybrid nanoparticles for simultaneous magnetofluorescent imaging and drug delivery. Angew Chem Int Ed Engl 2008;47:7284–8.
14. Chithrani BD, Ghazani AA, Chan WC. Determining the size and shape dependence of gold nanoparticle uptake into mammalian cells. Nano Lett 2006;6:662–8.
15. Maeda H. The enhanced permeability and retention (EPR) effect in tumor vasculature: the key role of tumor-selective macromolecular drug targeting. Adv Enzyme Regul 2001; 41:189–207.
16. Maki S, Konno T, Maeda H. Image enhancement in computerized tomography for sensitive diagnosis of liver cancer and semiquantitation of tumor selective drug targeting with oily contrast medium. Cancer 1985;56:751–7.
17. Fang J, Nakamura H, Maeda H. The EPR effect: unique features of tumor blood vessels for drug delivery, factors involved, and limitations and augmentation of the effect. Adv Drug Deliv Rev 2011;63:136–51.
18. Kaul G, Amiji M. Long-circulating poly(ethylene glycol)-modified gelatin nanoparticles for intracellular delivery. Pharm Res 2002;19:1061–7.
19. El-Sayed IH, Huang X, El-Sayed MA. Surface plasmon resonance scattering and absorption of anti-EGFR antibody conjugated gold nanoparticles in cancer diagnostics: applications in oral cancer. Nano Lett 2005;5:829–34.
20. Eghtedari M, Liopo AV, Copland JA, Oraevsky AA, Motamedi M. Engineering of hetero-functional gold nanorods for the in vivo molecular targeting of breast cancer cells. Nano Lett 2009;9:287–91.
21. Connor EE, Mwamuka J, Gole A, Murphy CJ, Wyatt MD. Gold nanoparticles are taken up by human cells but do not cause acute cytotoxicity. Small 2005;1:325–7.
22. Patra HK, Banerjee S, Chaudhuri U, Lahiri P, Dasgupta AK. Cell selective response to gold nanoparticles. Nanomedicine 2007;3:111–19.
23. Kirschenbaum J, Riesz P. Enhancement of 5-aminolevulinic acid-induced oxidative stress on two cancer cell lines by gold nanoparticles. Free Radic Res 2009;43:1214–24.
24. Pan Y, Leifert A, Ruau D, Neuss S, Bornemann J, Schmid G, et al. Gold nanoparticles of diameter 1.4 nm trigger necrosis by oxidative stress and mitochondrial damage. Small 2009; 5:2067–76.
25. Kang B, Mackey MA, El-Sayed MA. Nuclear targeting of gold nanoparticles in cancer cells induces DNA damage, causing cytokinesis arrest and apoptosis. J Am Chem Soc 2010;132:1517–19.
26. Hainfeld JF, Slatkin DN, Smilowitz HM. The use of gold nanoparticles to enhance radiotherapy in mice. Phys Med Biol 2004;49:N309–15.
27. Balasubramanian SK, Jittiwat J, Manikandan J, Ong CN, Yu LE, Ong WY. Biodistribution of gold nanoparticles and gene expression changes in the liver and spleen after intravenous administration in rats. Biomaterials 2010;31: 2034–42.
28. Patra CR, Bhattacharya R, Mukhopadhyay D, Mukherjee P. Fabrication of gold nanoparticles for targeted therapy in pancreatic cancer. Adv Drug Deliv Rev 2010;62:346–61.
29. Kullmann F, Hollerbach S, Dollinger M, Harder J, Fuchs M, Messmann H, et al. Cetuximab plus gemcitabine/oxaliplatin (GEMOXCET) in first-line metastatic pancreatic cancer: a multicentre phase II study. Br J Cancer 2009;100:1032–6.
30. Patra CR, Bhattacharya R, Wang E, Katarya A, Lau JS, Dutta S, et al. Targeted delivery of gemcitabine to pancreatic adenocarcinoma using cetuximab as a targeting agent. Cancer Res 2008;68:1970–8.
31. Jiang W, Kim BY, Rutka JT, Chan WC. Nanoparticle-mediated cellular response is size-dependent. Nat Nano 2008;3:145–50.
32. Issels RD, Lindner LH, Verweij J, Wust P, Reichardt P, Schem BC, et al. Neo-adjuvant chemotherapy alone or with regional hyperthermia for localised high-risk soft-tissue sarcoma: a randomised phase 3 multicentre study. Lancet Oncol 2010;11:561–70,
33. van der Zee J, González D, van Rhoon GC, van Dijk JDP, van Putten WLJ, Hart AAM. Comparison of radiotherapy alone with radiotherapy plus hyperthermia in locally advanced pelvic tumours: a prospective, randomised, multicentre trial. Lancet 2000;355:1119–25.
34. Vernon CC, Hand JW, Field SB, Machin D, Whaley JB, Van Der Zee J, et al. Radiotherapy with or without hyperthermia in the treatment of superficial localized breast cancer: results from five randomized controlled trials. Int J Radiation Oncol Biol Phys 1996;35:731–44.
35. Wust P, Hildebrandt B, Sreenivasa G, Rau B, Gellermann J, Riess H, et al. Hyperthermia in combined treatment of cancer. Lancet Oncol 2002;3:487–97.
36. Cherukuri P, Curley SA. Use of nanoparticles for targeted, noninvasive thermal destruction of malignant cells. Methods Mol Biol 2010;624:359–73.
37. Lal S, Clare SE, Halas NJ. Nanoshell-enabled photothermal cancer therapy: impending clinical impact. Acc Chem Res 2008;41:1842–51.
38. Hirsch L, Stafford R, Bankson J, Sershen S, Rivera B, Price R, et al. Nanoshell-mediated near-infrared thermal therapy of tumors under magnetic resonance guidance. PNAS 2003; 100:13549–54.
39. Stern JM, Stanfield J, Lotan Y, Park S, Hsieh JT, Cadeddu JA. Efficacy of laser-activated gold nanoshells in ablating prostate cancer cells in vitro. J Endourol 2007;21:939–43.
40. Stern JM, Cadeddu JA. Emerging use of nanoparticles for the therapeutic ablation of urologic malignancies. Urol Oncol 2008;26:93–6.
41. Essig M, Debus J, Schlemmer HP, Hawighorst H, Wannenmacher M, van Kaick G. Improved tumor contrast and delineation in the stereotactic radiotherapy planning of cerebral gliomas and metastases with contrast media-supported FLAIR imaging. Strahlenther Onkol 2000;176: 84–94.

42. Hainfeld JF, Slatkin DN, Focella TM, Smilowitz HM. Gold nanoparticles: a new X-ray contrast agent. Br J Radiol 2006;79:248–53.
43. Dwamena BA, Sonnad SS, Angobaldo JO, Wahl RL. Metastases from non-small cell lung cancer: mediastinal staging in the 1990s—meta-analytic comparison of PET and CT. Radiology 1999;213:530–6.
44. Vansteenkiste JF. FDG-PET for lymph node staging in NSCLC: a major step forward, but beware of the pitfalls. Lung Cancer 2005;47:151–3.
45. Vansteenkiste JF, Stroobants SG, De Leyn PR, Dupont PJ, Bogaert J, Maes A, et al. Lymph node staging in non-small-cell lung cancer with FDG-PET scan: a prospective study on 690 lymph node stations from 68 patients. J Clin Oncol 1998;16:2142–9.
46. Harisinghani MG, Barentsz J, Hahn PF, Deserno WM, Tabatabaei S, van de Kaa CH, et al. Noninvasive detection of clinically occult lymph-node metastases in prostate cancer. N Engl J Med 2003;348:2491–9.
47. Debouttiere PJ, Roux S, Vocanson F, Billotey C, Beuf O, Favre-Reguillon A, et al. Design of gold nanoparticles for magnetic resonance imaging. Adv Funct Mater 2006;16:2330–9.
48. Popovtzer R, Agrawal A, Kotov NA, Popovtzer A, Balter J, Carey TE, et al. Targeted gold nanoparticles enable molecular CT imaging of cancer. Nano Lett 2008;8:4593–6.
49. Alric C, Taleb J, Le Duc G, Mandon C, Billotey C, Le Meur-Herland A, et al. Gadolinium chelate coated gold nanoparticles as contrast agents for both X-ray computed tomography and magnetic resonance imaging. J Am Chem Soc 2008;130: 5908–15.
50. Cho SH. Estimation of tumour dose enhancement due to gold nanoparticles during typical radiation treatments: a preliminary Monte Carlo study. Phys Med Biol 2005;50: N163–73.
51. Spiers FW. The influence of energy absorption and electron range on dosage in irradiated bone. Br J Radiol 1949;22: 521–33.
52. Castillo MH, Button TM, Doerr R, Homs MI, Pruett CW, Pearce JI. Effects of radiotherapy on mandibular reconstruction plates. Am J Surg 1988;156:261–3.
53. Matsudaira H, Ueno AM, Furuno I. Iodine contrast medium sensitizes cultured mammalian cells to X rays but not to gamma rays. Radiat Res 1980;84:144–8.
54. Santos Mello R, Callisen H, Winter J, Kagan AR, Norman A. Radiation dose enhancement in tumors with iodine. Med Phys 1983;10:75–8.
55. Rose JH, Norman A, Ingram M, Aoki C, Solberg T, Mesa A. First radiotherapy of human metastatic brain tumors delivered by a computerized tomography scanner (CTRx). Int J Radiat Oncol Biol Phys 1999;45:1127–32.
56. Butterworth KT, Wyer JA, Brennan-Fournet M, Latimer CJ, Shah MB, Currell FJ, et al. Variation of strand break yield for plasmid DNA irradiated with high-z metal nanoparticles. Radiat Res 2008;170:381–7.
57. Carter JD, Cheng NN, Qu Y, Suarez GD, Guo T. Nanoscale energy deposition by X-ray absorbing nanostructures. J Phys Chem B 2007;111:11622–5.
58. Boudaiffa B, Cloutier P, Hunting D, Huels MA, Sanche L. Resonant formation of DNA strand breaks by low-energy (3 to 20 eV) electrons. Science 2000;287:1658–60.
59. Zheng Y, Hunting DJ, Ayotte P, Sanche L. Radiosensitization of DNA by gold nanoparticles irradiated with high-energy electrons. Radiat Res 2008;169:19–27.
60. Zheng Y, Sanche L. Gold nanoparticles enhance DNA damage induced by anti-cancer drugs and radiation. Radiat Res 2009;172:114–19.
61. Roeske JC, Nunez L, Hoggarth M, Labay E, Weichselbaum RR. Characterization of the theorectical radiation dose enhancement from nanoparticles. Technol Cancer Res Treat 2007;6:395–401.
62. McMahon SJ, Mendenhall MH, Jain S, Currell F. Radiotherapy in the presence of contrast agents: a general figure of merit and its application to gold nanoparticles. Phys Med Biol 2008;53:5635–51.
63. Garnica-Garza HM. Contrast-enhanced radiotherapy: feasibility and characteristics of the physical absorbed dose distribution for deep-seated tumors. Phys Med Biol 2009;54: 5411–25.
64. Cho SH, Jones BL, Krishnan S. The dosimetric feasibility of gold nanoparticle-aided radiation therapy (GNRT) via brachytherapy using low-energy gamma-/x-ray sources. Phys Med Biol 2009;54:4889.
65. Regulla DF, Hieber LB, Seidenbusch M. Physical and biological interface dose effects in tissue due to X-ray-induced release of secondary radiation from metallic gold surfaces. Radiat Res 1998;150:92–100.
66. Herold DM, Das IJ, Stobbe CC, Iyer RV, Chapman JD. Gold microspheres: a selective technique for producing biologically effective dose enhancement. Int J Radiat Biol 2000;76: 1357–64.
67. Chithrani DB, Jelveh S, Jalali F, van Prooijen M, Allen C, Bristow RG, et al. Gold nanoparticles as radiation sensitizers in cancer therapy. Radiat Res 2010;173:719–28.
68. Rahman WN, Bishara N, Ackerly T, He CF, Jackson P, Wong C, et al. Enhancement of radiation effects by gold nanoparticles for superficial radiation therapy. Nanomedicine 2009;5:136–42,
69. Hainfeld JF, Dilmanian FA, Zhong Z, Slatkin DN, Kalef-Ezra JA, Smilowitz HM. Gold nanoparticles enhance the radiation therapy of a murine squamous cell carcinoma. Phys Med Biol 2010;55:3045–59.
70. Zhang X, Xing JZ, Chen J, Ko L, Amanie J, Gulavita S, et al. Enhanced radiation sensitivity in prostate cancer by gold-nanoparticles. Clin Invest Med 2008;31:E160.
71. Kong T, Zeng J, Wang X, Yang X, Yang J, McQuarrie S, et al. Enhancement of radiation cytotoxicity in breast-cancer cells by localized attachment of gold nanoparticles. Small 2008;4:1537–43.
72. Roa W, Zhang X, Guo L, Shaw A, Hu X, Xiong Y, et al. Gold nanoparticle sensitize radiotherapy of prostate cancer cells by regulation of the cell cycle. Nanotechnology 2009;20: 375101,
73. Chien CC, Wang CH, Hua TE, Tseng PY, Yang TY, Hwu Y, et al. Synchrotron X-ray synthesized gold nanoparticles for tumour therapy, synchrotron radiation instrumentation: ninth international conference. 2007;1908–11.
74. Vaidya JS, Joseph DJ, Tobias JS, Bulsara M, Wenz F, Saunders C, et al. Targeted intraoperative radiotherapy versus whole breast radiotherapy for breast cancer (TARGIT-A trial): an international, prospective, randomised, non-inferiority phase 3 trial. Lancet 2010;376:91–102,
75. Morton GC. The emerging role of high-dose-rate brachytherapy for prostate cancer. Clin Oncol 2005;17:219–27.
76. Chithrani DB, Jelveh S, Jalali F, van Prooijen M, Allen C, Bristow RG, et al. Gold nanoparticles as radiation sensitizers in cancer therapy. Radiat Res 2010;173:719–28,
77. Liu CJ, Wang CH, Chen ST, Chen HH, Leng WH, Chien CC, et al. Enhancement of cell radiation sensitivity by pegylated gold nanoparticles. Phys Med Biol 2010;55:931–45.
78. Hebert EM, Debouttiere PJ, Hunting DJ, Lepage M, Sanche L. MRI detectable gadolinium-coated gold nanoparticles for radiotherapy. Int J Radiat Oncol Biol Phys 2008;72:S715–16.
79. Chang MY, Shiau AL, Chen YH, Chang CJ, Chen HH, Wu CL. Increased apoptotic potential and dose-enhancing effect of gold nanoparticles in combination with single-dose clinical electron beams on tumor-bearing mice. Cancer Sci 2008;99:1479–84.
80. Stern ST, Hall JB, Yu LL, Wood LJ, Paciotti GF, Tamarkin L, et al. Translational considerations for cancer nanomedicine. J Controlled Release 2010;146:164–74.

81. Libutti S, Paciotti G, Myer L, Haynes R, Gannon W, Walker M, et al. Results of a completed phase I clinical trial of CYT-6091: a pegylated colloidal gold-TNF. Nanomedicine 2009;27:3586.
82. Schiller JH, Storer BE, Witt PL, Alberti D, Tombes MB, Arzoomanian R, et al. Biological and clinical effects of intravenous tumor necrosis factor-alpha administered three times weekly. Cancer Res 1991;51:1651–8.
83. Paciotti GF, Myer L, Weinreich D, Goia D, Pavel N, McLaughlin RE, et al. Colloidal gold: a novel nanoparticle vector for tumor directed drug delivery. Drug Deliv 2004;11:169–83.
84. Libutti S, Paciotti G, Myer L, Haynes R, Gannon W, Walker M, et al. Results of a completed phase I clinical trial of CYT-6091: a pegylated colloidal gold-TNF. Nanomedicine 2009;27:3586,
85. Staves B. Pilot study of Aurolase™ therapy in refractory and/or recurrent tumors of the head and neck—full text view. Clinicaltrials.gov [homepage on the Internet]. Bethesda, MD: National Institutes of Health; 9 June 2010. Available from: http://clinicaltrials.gov/ct2/show/related/NCT00848042?term=auroshells&rank=1.
86. El-Sayed IH. Nanotechnology in head and neck cancer: the race is on. Curr Oncol Rep 2010;12:121–8.
87. Link S, El-Sayed MA. Size and temperature dependence of the plasmon absorption of colloidal gold nanoparticles. J Phys Chem B 1999;103:4212–17.